QUASI-PERIODIC HÉNON-LIKE ATTRACTORS IN 3D DIFFEOMORPHISMS

Henk W. Broer
Dept. of Mathematics
University of Groningen
The Netherlands
broer@math.rug.nl

Carles Simó
Dept. de Matemàtica Aplicada i Anàlisi
Universitat de Barcelona
Spain
carles@maia.ub.es

Renato Vitolo
Dip. di Matematica e Informatica
Università di Camerino
Italy
renato.vitolo@unicam.it

Abstract

The Hénon family of planar maps is considered driven by the Arnol′d family of circle maps. This leads to a five-parameter family of skew product systems on the solid torus. The dynamics of this skew product family and its perturbations are studied by numerical means. In certain parameter domains Hénon-like and quasi-periodic Hénon-like strange attractors are detected. The persistence properties of these attractors under perturbation of the skew-product structure of the map are discussed.

Key words

Attractors in 3D maps, quasi-periodic Hénon-like attractors, multiprecision numerical experiments, Lyapunov exponents.

1 Introduction

Since the 1990's several mathematical characterisations have been found concerning the structure of strange attractors in families of maps. A basic example is provided by the Hénon attractor [Hénon, 1976], occurring in the family of maps

$$H_{a,b} : \mathbb{R}^2 \to \mathbb{R}^2, \quad (x, y) \mapsto (1 - ax^2 + y,\, bx), \quad (1)$$

where a and b are real parameters. Benedicks and Carleson [Benedicks and Carleson, 1985; Benedicks and Carleson, 1991] proved that there exists a set of parameter values $\mathfrak{S}$, with positive Lebesgue measure, such that for all $(a, b) \in \mathfrak{S}$ the Hénon map $H_{a,b}$ (1) has a strange attractor coinciding with the closure $\mathrm{Cl}\,(W^u(p))$ of the unstable manifold of a saddle fixed point p. Here $\mathrm{Cl}\,(-)$ denotes the topological closure. Similar techniques were then used to prove occurrence of strange attractors in parameterised families of maps, near homoclinic tangencies in two or higher dimensions [Mora and Viana, 1993; Palis and Viana, 1994; Tatjer, 2001; Viana, 1993], and near tangencies in the saddle-node critical case [Díaz, Rocha and Viana, 1996]. See [Wang and Young, 2001] for a general set-up to prove existence of strange attractors with one positive Lyapunov exponent in families of two-dimensional maps. The strange attractors considered in these references are called *Hénon-like* [Díaz, Rocha and Viana, 1996; Mora and Viana, 1993; Viana, 1993].

1.1 Setting of the problem

In this paper we perform a numerical study of certain model map families, searching these for Hénon-like attractors as well as for so-called *quasi-periodic Hénon-like* attractors. A basic model for this study is the family of maps of the solid torus $\mathbb{R}^2 \times \mathbb{S}^1$, where $\mathbb{S}^1 = \mathbb{R}/\mathbb{Z}$ is the circle, given by

$$\begin{pmatrix} x \\ y \\ \theta \end{pmatrix} \mapsto \begin{pmatrix} 1 - (a + \varepsilon \sin(2\pi\theta))x^2 + y \\ bx \\ \theta + \alpha + \delta \sin(2\pi\theta) \end{pmatrix}, \quad (2)$$

where both (ε, δ) are perturbation parameters. This map is a skew product perturbation of the Hénon map (1) by the Arnol′d family [Arnol′d, 1965]

$$A_{\alpha,\delta} : \mathbb{S}^1 \to \mathbb{S}^1, \quad \theta \mapsto \theta + \alpha + \delta \sin(2\pi\theta). \quad (3)$$

First let us consider the uncoupled situation $\varepsilon = 0$. The dynamics of the Arnol′d family is well-understood and that of the Hénon family is partially known. For the Arnol′d family, in the (α, δ)-plane there is a countable union of resonance tongues [Arnol′d, 1965; Broer, Simó and Tatjer, 1998] with non-empty interior, corresponding to hyperbolic periodic dynamics. In the complement, which is of positive measure, quasi-periodic dynamics [Arnol′d, 1965; Broer, Huitema and Sevryuk, 1996] takes place, see Figure 1. Similarly, for the Hénon family in the (a, b)-plane there exists

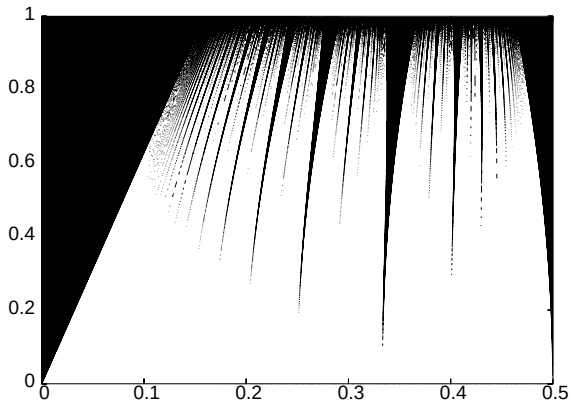

Figure 1. Organisation of the (α, δ)-parameter plane of the Arnol′d family (3) by resonance tongues, containing an open set with periodic dynamics (indicated in black). The remaining parameter values (indicated in white) form a nowhere dense set of positive measure with quasi-periodic dynamics.

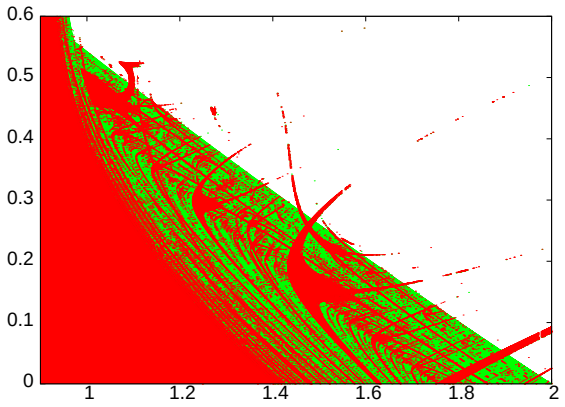

Figure 2. Organisation of the (a, b)-parameter plane of the Hénon family (1) by strips with periodic dynamics and crossroad areas (in red). A complement of positive measure contains strange attractors (in green). The upper right part of the diagram (in white) corresponds to escape.

a countable union of strips of non-empty interior corresponding to hyperbolic periodic dynamics. In the complement, a set of positive measure corresponds to strange attractors [Benedicks and Carleson, 1991]. Most of the strips are extremely narrow and only become visible when they intersect another strip of the same period in such a way that a "crossroad area" is created [Bosch, Carcassès, Mira and Tatjer, 1991]. See Figure 2.

Remark 1. *Figures* 1, 2, *and* 3 *are mostly obtained by numerical computation of Lyapunov exponents* [Simó, 2003]. *See Section* 2 *for a description of the procedure and Section* 3 *for the interpretation of the Lyapunov exponents in terms of the dynamics. Figure* 2 *uses the origin as initial point, which can land either in a periodic sink, or on a strange attractor or can escape 'to infinity'. Notice that, due to multistability other initial points can tend to different attractors. Moreover, some of the periodicity strips are connected to windows of sinks of the logistic family as this occurs for* $b = 0$.

To fix ideas, consider map (2) in the uncoupled case $\varepsilon = 0$. There are at least four combinations of the dynamics of the Arnol′d and Hénon families that correspond to parameter domains of positive measure.

1. We start considering the case where the Hénon family is in a periodic attractor, so where the (maximal) Lyapunov exponent $\Lambda_H < 0$. Then the maximal Lyapunov exponent Λ_A of the Arnol′d family may be negative or zero.
   (a) The case $\Lambda_A < 0$ is the most simple. Parameters (α, δ, a, b) are such that both maps $A_{\alpha,\delta}$ and $H_{a,b}$ are in a hyperbolic periodic attractor. In the solid torus $\mathbb{R}^2 \times \mathbb{S}^1$ this also gives a hyperbolic periodic attractor for map (2).
   (b) If $\Lambda_A = 0$, the Arnol′d family is quasi-periodic, while the Hénon family is in a periodic attractor. The corresponding uncoupled dynamics of map (2) is a normally hyperbolic (attracting) quasi-periodic invariant circle.
2. In the two remaining cases the Hénon family is in a strange attractor, so with $\Lambda_H > 0$. This attractor is the closure $\mathrm{Cl}\,(W^u(\mathrm{Orb}(p)))$ of the unstable manifold of a periodic orbit of saddle type, see [Benedicks and Carleson, 1985; Benedicks and Carleson, 1991; Díaz, Rocha and Viana, 1996; Mora and Viana, 1993; Viana, 1993]. We have to distinguish two cases.
   (a) The Arnol′d family is in a periodic attractor, so with $\Lambda_A < 0$, and the product system has a Hénon-like attractor. For illustrations see Figure 4.
   (b) The Arnol′d family is quasi-periodic, so with $\Lambda_A = 0$, and the Hénon map has a strange

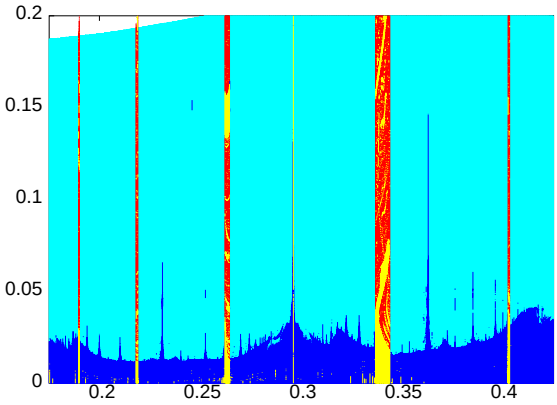

Figure 3. Diagram of map (2) in the (α, ε)-plane, for $a = 1.25, b = 0.3$ and $\delta = 0.6/(2\pi)$. Visible are: domains which can be interpreted as having periodic attractors (code 1, yellow), quasi-periodic attractors (code 2, blue), Hénon-like attractors (code 3, red) and quasi-periodic Hénon-like attractors (code 4, light blue). The diagram is obtained by examining the Lyapunov exponents of (2). See Sections 2 and 3 for details.

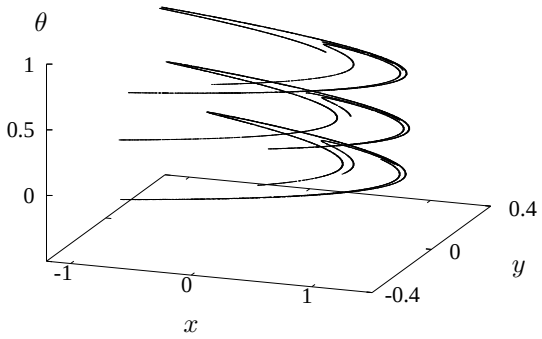

Figure 4. Hénon-like strange attractor of the family (2) for (α, δ) in an Arnol′d tongue of period three. Parameters are fixed at $a = 1.3$, $b = 0.3$, $\varepsilon = 0.2$, $(\alpha, \delta) = (0.33793, 0.116)$.

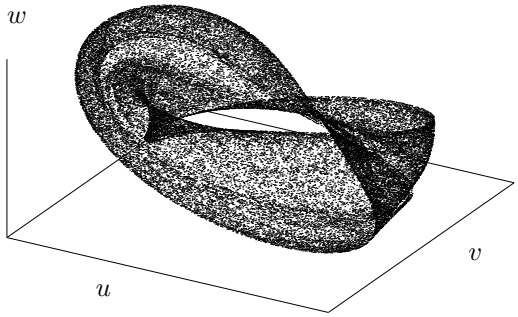

Figure 5. Quasi-periodic Hénon-like strange attractor of the model family (2). Parameter values are fixed at $a = 1.85$, $b = -0.2$, $\delta = 0$, $\alpha = (\sqrt{5} - 1)/2$, $\varepsilon = 0.1$. For a better visualisation of the folds, the plot is given in the variables (u, v, w), where $u = (r+4)\cos(\theta)$, $v = (r+4)\sin(\theta)$, with $r = x\cos(\theta)+10y\sin(\theta)$, and $w = -x\sin(\theta)+10y\cos(\theta)$.

> attractor. The uncoupled product dynamics is said to be quasi-periodic Hénon-like, *i.e.*, on a strange attractor of the form $\mathrm{Cl}\left(W^u(\mathscr{C})\right)$, where $\mathscr{C}$ is a quasi-periodic invariant circle of saddle-type.

The Lyapunov diagram in Figure 3 strongly suggests that all four cases persist for $\varepsilon \neq 0$, $|\varepsilon| \ll 1$, in parameter sets of positive measure. More concretely, case 1(a) corresponds to code 1; case 1(b) to code 2; case 2(a) to code 3, and case 2(b) to code 4.

Persistence of the periodic attractors (case 1(a)) follows from the theory of normally hyperbolic invariant manifolds [Hirsch, Pugh and Shub, 1977]. Persistence of the attracting quasi-periodic invariant circles (case 1(b)) is proved in [Broer, Simó, Vitolo, 2005, Theorem 3], by applying KAM theory [Broer, Huitema and Sevryuk, 1996; Broer, Huitema, Takens and Braaksma, 1990]. Persistence of Hénon-like strange attractors (case 2(a)) for $|b|, |\varepsilon| \ll 1$ is proved in [Broer, Simó, Vitolo, 2005], where partial results concerning quasi-periodic Hénon-like attractors (case 2(b)) are shown.

The main focus of this paper is to study persistence properties of quasi-periodic Hénon-like attractors for small ε. See Figure 5 for an illustration of a quasi-periodic Hénon-like attractor.

1.2 Motivation

Quasi-periodic Hénon-like attractors have been conjectured to occur in diffeomorphisms of $\mathbb{R}^3 = \{x, y, z\}$, obtained as Poincaré return maps for a climatological model [Broer, Simó and Vitolo, 2002; Broer, Simó and Vitolo, 2003; Vitolo, 2003], like the attractor $\mathscr{A}$ displayed in Figure 6. Examination of a cross-section Σ of the attractor (magnified in Figure 6 (B)) suggests that $\mathscr{A}$ is contained in a two-dimensional manifold which is folded onto itself, in analogy with the structure of the Hénon attractor [Hénon, 1976]. This manifold is conjectured to be the unstable manifold $W^u(\mathscr{C})$ of a quasi-periodic invariant circle $\mathscr{C}$ of saddle type. To illustrate the dynamics inside $\mathscr{A}$ we computed the image of the slice Σ under the return map. This yields a folded curve looking like a planar Hénon attractor.

Also we mention that the occurrence of strange attractors which look similar to Figure 5 is observed in [Glendinning, 1998; Grebogi, Ott, Pelikan and Yorke, 1984; Keller, 1996; Osinga and Feudel, 2000; Osinga, Wiersig, Glendinning and Feudel, 2001]. Although most of these studies deal with endomorphisms of the interval forced by a rigid rotation in a skew product way, and some of them have negative Lyapunov exponents (beyond the one trivially equal to zero), a relationship with the present approach is discussed later on.

The theoretical knowledge of attractors in dimension higher than 2 is limited. As positive exceptions to this we mention Viana [Viana, 1993; Viana, 1997], Tatjer [Tatjer, 2001], Wang & Young [Wang and Young, 2001] and Gonchenko et al. [Gonchenko, Ovsyannikov, Simó and Turaev, 2005]. The Hénon-like attractors found in the present paper, to some extent, also belong to this domain. In this sense one may say that the understanding of the quasi-periodic Hénon-like attractor is a next step in this research program. This led us to examine model maps such as (2), that combine quasi-periodic and Hénon-like dynamics.

1.3 Summary and outline

This paper contains a numerical study of map (2) and of a more general model, given by

$$\mathcal{T} = \mathcal{T}_{\alpha,\delta,a,b,\varepsilon,\mu} : \mathbb{R}^2 \times \mathbb{S}^1 \to \mathbb{R}^2 \times \mathbb{S}^1,$$
$$\begin{pmatrix} x \\ y \\ \theta \end{pmatrix} \mapsto \begin{pmatrix} 1 - (a + \varepsilon \sin(2\pi\theta))x^2 + y \\ bx \\ \theta + \alpha + \delta \sin(2\pi\theta) + \mu y \end{pmatrix}, \quad (4)$$

depending on the six parameters $(\alpha, \delta, a, b, \varepsilon, \mu)$.

Remark 2. *Maps* (4) *and* (2) *are identical except for the term* μy*. In fact, map* (4) *is a 'fully coupled' version of* (2)*, where the skew-product structure is perturbed by*

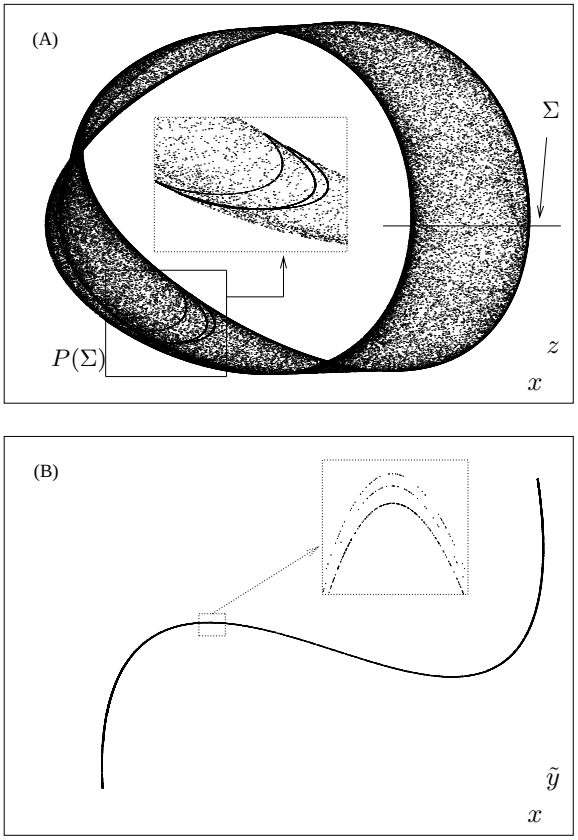

Figure 6. (A) Strange attractor $\mathscr{A}$ of the Poincaré return map of a climatological system [Broer, Simó and Vitolo, 2002]. Compare with Figure 5. The attractor $\mathscr{A}$ is plotted with a 'slice' Σ and with the image of Σ under the return map. The slice Σ contains all points with distance less that 0.0001 from the plane $z = 0$. The image of $\Sigma$is magnifi ed in the central box. (B) Slice Σ of the attractor $\mathscr{A}$ in (A), projection on the $(x, \tilde{y})$-plane, with $\tilde{y} = y - 0.133 * z$.

the term μy. The distinction in two maps is kept for the sake of clarity. In the sequel we often refer to (2) *as the 'skew case' and to* (4) *as the 'fully coupled case'.*

The results, presented in Section 3, are related to the subdivision in four classes of dynamics as given in Section 1.1 in the uncoupled setting $\mu = \varepsilon = 0$. Main focus is on the persistence of quasi-periodic Hénon-like attractors for map (2) when $\varepsilon \neq 0$ and for map (4) when both ε and μ are nonzero. A few theoretical results are quoted from [Broer, Simó, Vitolo, 2005], in order to complete the dynamical picture. To clarify the discussion, we begin by describing the numerical procedures and by explaining our choices for the parameter values, see next section.

2 Numerical methods and selection of parameter values

In the present study of family $\mathcal{T}$ (4) several parameters have been kept fixed. We chose $\delta = 0.6/(2\pi)$, so that resonant zones of the Arnol′d family (3) are not too narrow, while still most of the values of α give rise to quasi-periodic dynamics. Concerning the parameters a and b of the Hénon family (1), we fixed $b = 0.3$ for historical reasons. It is the value used by Hénon [Hénon, 1976], and it is a good compromise between dissipation and visibility of the folds of the unstable manifold $W^u(p)$ (compare the discussion in Section 1). It was also used in [Simó, 1979] to study attractors as well as homoclinic and heteroclinic tangencies (later on in the literature renamed as 'crises'). The value $a = 1.25$ corresponds to a periodic attractor of period 7 and allows for moderate values of ε in the forcing before escape occurs. Finally we selected the values $\mu = 0$ and $\mu = 0.01$ for the skew (2) and the fully coupled case (4), respectively.

Diagrams such as that in Figure 3 are obtained by computing an orbit of map (2) and examining the three Lyapunov exponents $\Lambda_1 \geq \Lambda_2 \geq \Lambda_3$. The latter are computed from the so-called *Lyapunov sums* as follows (also see [Simó, 2003]).

Let T be a three-dimensional map and consider an orbit $\{x_j = T^j(x_0), j = 0, 1, 2, 3, \ldots\}$. Three linearly independent tangent vectors (v_0, w_0, z_0) are selected and their images under the derivative DT^n along the orbit $\{x_j\}$ are computed, where Gram-Schmidt orthnormalisation is performed every step (or every $m > 1$ steps to speed up the procedure). Let $\hat{v}_1 = DT(x_0)v_0$. Define $f_1 = \|\hat{v}_1\|$ and $v_1 = \hat{v}_1/f_1$. The remaining two vectors are orthonormalised as follows: define $g_1 = \|w_1'\|$, where

$$w_1' = \hat{w}_1 - (v_1 \cdot \hat{w}_1)v_1 \quad \text{and} \quad \hat{w}_1 = DT(x_0)w_0,$$

and put $w_1 = w_1'/g_1$. Similarly for z_1, yielding a coefficient h_1. The procedure is iterated, thus obtaining three sequences f_j, g_j, h_j, $j \geq 1$. The Lyapunov sums are then defined as

$$LS_n^1 = \sum_{j=1}^{n} \log(f_j),$$
$$LS_n^2 = \sum_{j=1}^{n} \log(g_j),$$
$$LS_n^3 = \sum_{j=1}^{n} \log(h_j).$$

The maximal Lyapunov exponent Λ_1 is given by the average slope of the Lyapunov sum LS_n^1 as $n \to \infty$, that is, the average of the logarithmic rates of increase of the length $\log(f_j)$. The other two Lyapunov exponents Λ_2, Λ_3 are obtained in the same way from LS^2 and LS^3 respectively.

In the numerical procedure, estimates are produced of the average slope of LS_j^k for $j = 1, \ldots, n$ for different values of n up to a maximal number N of iterates. The computation is stopped before N iterates in case of escape, or if a periodic orbit is detected, or if different

estimates of the average coincide within a prescribed tolerance ρ. Typical values for N and ρ in the present computations are 10^7 and 10^{-6}, respectively.

The values of the Lyapunov exponents are used to determine the types of attractor occurring in different parameter regions. For example, attracting invariant circles (or periodically invariant circles) are characterised by a zero maximal Lyapunov exponent. In particular, with the above choice of parameter values, for the skew-product map (2) one may expect to have a period 7 attracting invariant circle if (α, δ) is in the quasi-periodic domain and ε is sufficiently small, compare Figure 3.

However, in some cases we are forced to use the following complementary tool to help decide whether the attractor is a quasi-periodic circle or not (this is often necessary for map (2) when ε is small). After some transient, the points of an orbit of map (2) (or of some power of it) are sorted by the values of θ. If the attractor is an invariant circle $(x(\theta), y(\theta))$, then the variation of the components (x, y) can be estimated from the iterates along the orbit. This variation has to remain bounded when the number of iterates increases and must converge to the true variation. This procedure may fail as well, as reported in the next section.

3 The dynamics of the model maps: numerical observations

The diagram in Figure 3 is based on the values of the two largest Lyapunov exponents Λ_1 and Λ_2, $\Lambda_1 \geq \Lambda_2$. To be more precise, code 1 (yellow) corresponds to $0 > \Lambda_1$, code 2 (blue) to $0 = \Lambda_1 > \Lambda_2$, code 3 (red) to $\Lambda_1 > 0 > \Lambda_2$ and code 4 (light blue) to $\Lambda_1 > 0 = \Lambda_2$. Typically we considered a Lyapunov exponent as equal to zero whenever $|\Lambda_j| < 10^{-5}$, $j = 1, 2$.

The above codes have the following interpretation in terms of dynamics: code 1 corresponds to a periodic sink, code 2 to a quasi-periodic attracting invariant circle, code 3 to a Hénon-like attractor and code 4 to a quasi-periodic Hénon-like attractor. Compare the four classes of dynamics of map (2) described for $\varepsilon = 0$ in Section 1.

Notice that the role of Λ_3 is not very relevant. It can only help to decide, in case of periodic or quasi-periodic attractors, whether the normal behaviour is of nodal type ($\Lambda_2 > \Lambda_3$) or of focal type ($\Lambda_2 = \Lambda_3$). The major role is played by Λ_1 and Λ_2 and their position with respect to zero.

We now describe the dynamics of map (2) in more detail, referring to Figure 3. Varying α with δ fixed at $0.6/(2\pi)$ means that the driving Arnol′d family (3) crosses several resonance tongues, along a horizontal line in Figure 1. Inside each of these tongues, the dynamics of (3) is 'phase-locked' to a periodic attractor. The Hénon family (1) also has a periodic attractor for the selected parameter values (see previous section). Therefore, map (2) has a periodic attractor inside the Arnol′d tongues for $\varepsilon = 0$.

By normal hyperbolicity [Hirsch, Pugh and Shub, 1977], the periodic attractor is expected to persist for small ε. This is confirmed by Figure 3 (yellow regions, code 1). Due to the skew-product structure of (2), the resonance tongues of (3) are not affected by increasing ε. However, the periodic attractor of (2) ceases to exist for larger values of ε and a Hénon-like strange attractor appears inside the tongues (red spots, code 2).

For α outside all Arnol′d tongues the dynamics of (3) is quasi-periodic. This corresponds to a quasi-periodic circle attractor of (2) at $\varepsilon = 0$. By [Broer, Simó, Vitolo, 2005, Theorem 3] this attractor persists for small ε. Compare the dark blue parameter domains in Figure 3, code 3. For larger values of ε quasi-periodic Hénon-like attractors occur, in a relatively large part of the parameter plane (code 4, light blue). We now examine the dynamics of map (4), where the skew-product structure of (2) is perturbed by putting $\mu = 0.01$. Figure 7 contains a diagram for map (4) produced in the same way and for the same parameter values as Figure 3.

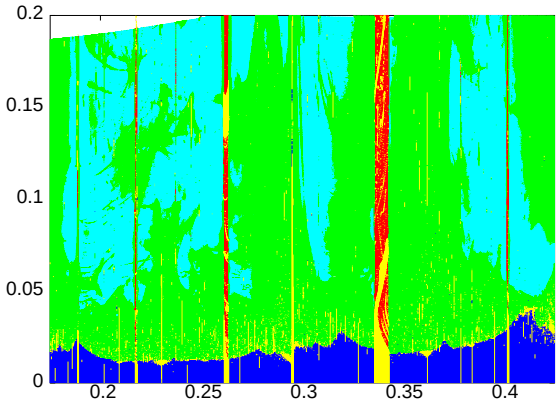

Figure 7. Diagram of the fully coupled system (4) in the (α, ε)-plane, for $a = 1.25, b = 0.3, \mu = 0.01$ and $\delta = 0.6/(2\pi)$. According to the values of the Lyapunov exponents, we interpret as follows: domains of periodic attractors (code 1, yellow), of quasi-periodic attractors (code 2, blue), of Hénon-like attractors (code 3, red) and of 'quasi-periodic Hénon-like' attractors (codes 4, light blue, and 5, green).

A remarkable difference between the skew-product case (2) and the fully coupled case (4) is that a zero Lyapunov exponent practically never occurs for the latter map. Indeed, any small perturbation $\mu \neq 0$ has the effect of shifting the value of Λ_2 away from zero. Its modulus remains small, but the sign may be either positive or negative, and both cases occur. This roughly happens for those regions of the (α, ε)-parameter plane which, in the skew case $\mu = 0$ seemingly show quasi-periodic Hénon-like attractors (code 4 regions in Figure 3).

Therefore a new case appears for $\mu \neq 0$, namely $\Lambda_1 > \Lambda_2 > 0$. Here the value of Λ_2 is small but definitely positive. For these parameter values we maintain

the code 4 (light blue) in Figure 7. (The existence of parameter values for which the two largest Lyapunov exponents are positive has been recently also found in a quite different context, related to what can be considered as a discrete version of Lorenz attractor, see [Gonchenko, Ovsyannikov, Simó and Turaev, 2005].)

Furthermore, in the case $\Lambda_1 > 0 > \Lambda_2$, where Λ_2 is close to zero but definitely negative, one has to distinguish two possibilities. There are Hénon-like attractors such that the θ-component is not periodic (this was the case for map (2)). These are identified by the property that the angular component θ of the iterates should cluster around the periodic attractor of (3) obtained in the case $\mu = 0$. For these we keep the code 3 (red) in Figure 7. The remaining cases with Λ_2 negative and close to zero can be seen as a perturbation of the quasi-periodic Hénon attractors occurring at $\varepsilon = 0$. For these the code 5 (green) is used.

Comparing Figures 3 and 7 we observe:

1) Regions with code 1 (periodic attractors, yellow) in Figure 3 is essentially preserved in Figure 7. In the latter, more periodic attractors are detected near the parameter regions that in the skew case correspond to resonance.
2) Regions with code 3 (Hénon-like attractors, red) are quite similar in both figures.
3) The region with code 4 in Figure 3 (quasi-periodic Hénon attractors, light blue), roughly splits in two regions in Figure 3, with codes 4 (light blue) and 5 (green) respectively. The difference is given by the sign of Λ_2: positive in region 4, negative in region 5, but always close to zero.
4) The region with code 2 (blue) in Figure 3, where $\Lambda_1 = 0 > \Lambda_2$ is reduced in size in Figure 7: for ε sufficiently far from 0, several 'blue' points for $\mu = 0$ turn into green ($\Lambda_1 > 0 > \Lambda_2$) when $\mu = 0.01$.

Concerning the last point, one may expect that, for those parameter values, the dynamics in the skew case $\mu = 0$ has a quasi-periodic attractor. In fact, the numerical evidence *in double precision arithmetics*, shows a different kind of attractors. In the literature these are called 'strange non-chaotic attractors' (SNA). See [Grebogi, Ott, Pelikan and Yorke, 1984; Keller, 1996; Glendinning, 1998; Osinga and Feudel, 2000; Osinga, Wiersig, Glendinning and Feudel, 2001; Jorba and Tatjer, 2005] for examples and theoretical results in various contexts.

As explained in Section 2 one can use the variation as an indicator to distinguish an invariant circle from invariant sets of other types. In the skew case this method reveals a large domain on the upper part of the blue region, which seems to be characterised by the presence of SNAs. This is illustrated in Figure 8, that contains magnifications of both Figures 3 and 7 for $\varepsilon \in [0, 0.05]$. Parameter values characterised by "SNAs" are represented by colour magenta (code 6) in Figure 8. This is particularly evident near the resonance tongue with

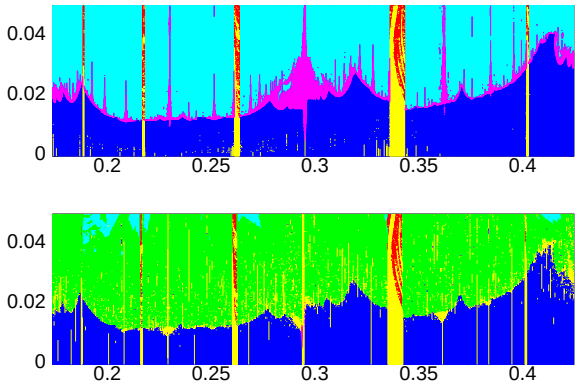

Figure 8. Magnified domain of Figures 3 (top) and 7 (bottom). In the top figure a new code 6 (in magenta) is introduced, roughly located above the blue region. In Figure 3 this magenta domain was shown in blue. It apparently corresponds to "strange non-chaotic attractors". See the text for explanation and discussion.

rotation number $2/7$. Narrow domains can be observed near other resonances.

In fact, it turns out that a naive application of the variation criterion may fail to give correct results. The "SNAs" detected by this method can be an artifact of finite numerical precision in the computations. See the next section and compare with [Broer, Simó, Vitolo, 2005].

4 Interpretation of the results

Theoretical results from [Broer, Simó, Vitolo, 2005] confirm a large part of the numerical study described in the previous section. In particular, by a KAM-like Theorem in the dissipative setting [Broer, Simó, Vitolo, 2005, Theorem 3], existence of quasi-periodic attractors for map (4) is proved for small ε, μ .

By comparing top and bottom part of Figure 8, we observe that most parameter values corresponding to quasi-periodic attractors for $\mu = 0$ remain blue (code 2) for $\mu = 0.01$. This suggests that the parameter domain of validity of the above KAM-like Theorem is relatively large.

It is striking that essentially all parameter values with code 6 in Figure 8 (say, candidates for "SNA" in the skew case), enter into the 'green region' (code 5, $\Lambda_1 > 0 > \Lambda_2$) for $\mu = 0.01$. This behaviour has been further checked by varying μ for a sample of values of (α, ε) : even when μ is as small as 10^{-12} a positive maximal Lyapunov exponent has been detected.

To clarify this lack of persistence of "SNAs", a careful numerical study of a few 'toy models' is performed in [Broer, Simó, Vitolo, 2005]. One of the models used there is the map of the cylinder $\mathbb{R} \times \mathbb{S}^1$ given by

$$(x, \theta) \mapsto (1 - (a + \varepsilon \sin(2\pi\theta))x^2, \theta + \alpha), \quad (5)$$

that is, the logistic family driven by a rigid rotation. Computations are performed both in double precision

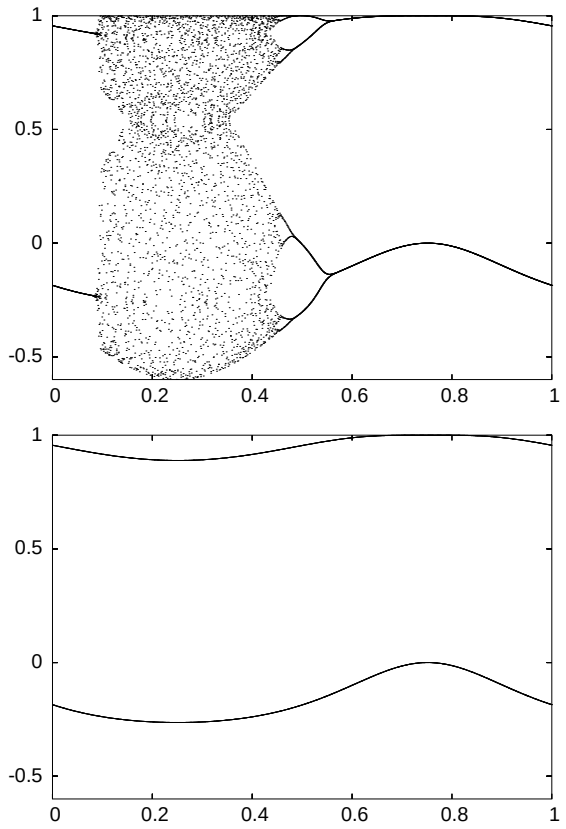

Figure 9. Attractors observed for map (5) with $(a, \varepsilon, \alpha) = (1.30, 0.30, \gamma/1000)$, where γ denotes the golden mean. Top: standard double precision arithmetics is used, yielding an "SNA". Bottom: 150-decimal digits arithmetics is used.

and with 150 decimal digits, for the same parameter values and initial conditions. The computed attractors are "SNAs" in the first case and smooth invariant circles in the second, see Figure 9.

As it is exhaustively clarified in [Broer, Simó, Vitolo, 2005], this phenomenon is due to the occurrence, locally in θ, of strong expanding normal behaviour of the invariant circle, whereas the average normal behaviour is contracting. This brings into serious doubt the occurrence of SNAs in the family (2), and motivates our use of quotes when speaking about "SNAs".

Persistence of Hénon-like attractors in family (2) follows from [Broer, Simó, Vitolo, 2005, Theorem 4]. In particular, it is shown that Hénon-like attractors occur for a positive measure set of parameter values, when ε and b are sufficiently small. This corresponds to red (code 3) in Figure 3. Occurrence of Hénon-like attractors for larger values of ε and b and for map (4) when $\mu \neq 0$ remains conjectural and based on the numerical evidence.

Also conjectural is the existence of quasi-periodic Hénon-like attractors in maps (2) and (4). For both maps, by [Broer, Simó, Vitolo, 2005, Theorem 1] we expect that the attractor is *contained in* the closure $\mathrm{Cl}\,(W^u(\mathscr{C}))$ of a quasi-periodic invariant circle $\mathscr{C}$ of saddle-type. However, we do not know on theoretical grounds whether the attractor is *equal to* the closure $\mathrm{Cl}\,(W^u(\mathscr{C}))$ and whether a dense orbit exists with a positive Lyapunov exponent.

We mention another point that should be clarified, even from the numerical point of view, about the quasi-periodic Hénon-like attractors. No visual differences can be observed between these attractors in the three cases $\Lambda_2 = 0$, $\Lambda_2 < 0$ and $\Lambda_2 > 0$. Recall that the first case occurs for $\varepsilon = 0$ (map (2)), whereas either the second or the third occur whenever $\mu \neq 0$.

Figure 10 displays the attractor detected for $(\alpha, \varepsilon, \mu) = (0.31, 0.13, 0.01)$ (in the region of code 4 in Figure 7). The plot uses variables (u, v, w) analogous to Figure 5. Moving the parameters to $(\alpha, \varepsilon, \mu) = (0.28, 0.13, 0.01)$ (code 5 region in Figure 7) or to $(\alpha, \varepsilon, \mu) = (0.28, 0.13, 0.00)$ (code 4 region in Figure 3), the detected attractor looks quite similar to Figure 10. Further study is needed to clarify the geometric differences in the three cases, by considering the unstable manifold of the invariant circle of saddle type which is expected to occur.

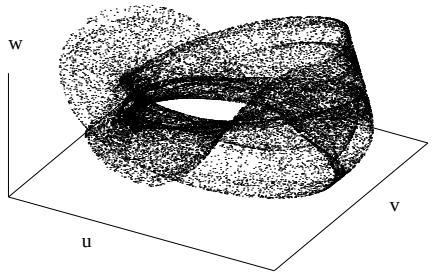

Figure 10. Attractor of $\mathcal{T}$ as in (4) for $(\alpha, \varepsilon, \mu) = (0.31, 0.13, 0.01)$, with two positive Lyapunov exponents: $\Lambda_1 \approx 0.29530$ and $\Lambda_2 \approx 0.00016$. No visual difference is observed in the structure of attractors having Λ_2 negative and close to zero (fully coupled case $\mu > 0$) and attractors with $\Lambda_2 = 0$ (skew product case $\mu = 0$, map (2)). The representation uses variables (u, v, w) similar to Figure 5.

5 Conclusion

A numerical study is performed of a model map which is constructed in such a way as to combine quasi-periodic and chaotic dynamics. The model map is a perturbation of the product of the Arnol′d family of maps of the circle times the planar Hènon family, and it depends on several parameters.

Main tool in the present investigation is the computation of Lyapunov exponents on orbits belonging to attractors of the model map. Large regions in the considered parameter domains are characterised by attractors of *quasi-periodic Hénon-like* type. For such attractors,

in the skew product case (Arnol′d family unperturbed) a positive and a zero Lyapunov exponents are detected. After perturbation of skewness, either two positive or one positive and one negative Lyapunov exponents are detected. It remains to be clarified which other geometrical and dynamical features differentiate the latter two cases from the skew product situation.

Moreover, for certain parameter values in the skew case it is necessary to use high precision arithmetics to obtain reliable results. Indeed, attractors that, in double precision, mistakingly look 'strange nonchaotic', turn out to be smooth invariant circles.

Acknowledgements

The authors are indebted to Henk Bruin, Àngel Jorba, Marco Martens, Vincent Naudot, Floris Takens, Joan Carles Tatjer and Marcelo Viana for valuable discussion. The first author is indebted to the Departament de Matemàtica Aplicada i Anàlisi, Universitat de Barcelona, for hospitality and the last two authors are indebted to the Department of Mathematics, University of Groningen, for the same reason. The research of C.S. has been supported by grants DGICYT BFM2003-09504-C02-01 (Spain) and CIRIT 2001 SGR-70 (Catalonia). Work of R.V. has been partially supported by MIUR PRIN Grant "Gli estremi meteo-climatici nell'area mediterranea: proprietà statistiche e dinamiche", Italy. The computing cluster HIDRA of the UB Group of Dynamical Systems have been widely used. We are indebted to J. Timoneda for keeping it fully operative.

References

Arnol′d, V.I. (1965). Small denominators, I: Mappings of the circumference into itself. *AMS Transl. (Ser. 2)* **46**, pp. 213–284.

Benedicks, M. and Carleson, L. (1985). On iterations of $1 - ax^2$ on $(-1, 1)$. *Ann. of Math. (2)* **122(1)**, pp. 1–25.

Benedicks, M. and Carleson, L. (1991). The dynamics of the Hénon map. *Ann. of Math. (2)* **133(1)**, pp. 73–169.

Bosch, M., Carcassès, J.P., Mira, C., Simó, C. and Tatjer, J.C. (1991). "Crossroad area-spring area" transition. (I) Parameter plane representation. *Int. J. of Bifurcation and Chaos* **1(1)**, pp. 183–196.

Broer, H.W., Huitema, G.B. and Sevryuk, M.B. (1996). *Quasi-periodic Motions in Families of Dynamical Systems, Order amidst Chaos*. Springer LNM **1645**.

Broer, H.W., Huitema, G.B., Takens, F. and Braaksma, B.L.J. (1990). Unfoldings and bifurcations of quasi-periodic tori. *Mem. AMS* **83(421)**, pp. 1–175.

Broer, H.W., Simó, C. and Tatjer, J.C. (1998). Towards global models near homoclinic tangencies of dissipative diffeomorphisms. *Nonlinearity* **11** pp. 667–770.

Broer, H.W., Simó, C. and Vitolo, R. (2002). Bifurcations and strange attractors in the Lorenz-84 climate model with seasonal forcing. *Nonlinearity* **15(4)**, pp. 1205–1267.

Broer, H.W., Simó, C. and Vitolo, R. (2003). Quasi-periodic Hénon-like attractors in the Lorenz-84 climate model with seasonal forcing. *Proceedings Equadiff 2003*.

Broer, H.W., Simó, C. and Vitolo, R. (2005). Chaos and quasi-periodicity in diffeomorphisms of the solid torus. Preprint **mp_arc** # 05-107.

Díaz, L., Rocha, J. and Viana, M. (1996). Strange attractors in saddle cycles: prevalence and globality. *Inv. Math.* **125**, pp. 37–74.

Glendinning, P. (1998). Intermittency and strange nonchaotic attractors in quasi-periodically forced circle maps. *Phys. Lett. A* **244**, pp. 545–550.

Gonchenko, S.V., Ovsyannikov, I.I., Simó, C. and Turaev, D. (2005). Three-dimensional Hénon maps and wild Lorenz–like attractors. Preprint **mp_arc** # 05-111.

Grebogi, C., Ott, E., Pelikan, S. and Yorke, J. (1984). Strange attractors that are not chaotic. *Physica D* **13(1-2)**, pp. 261–268.

Hénon., M (1976). A two dimensional mapping with a strange attractor. *Comm. Math. Phys.* **50**, pp. 69–77.

Hirsch, M.W., Pugh, C.C. and Shub, M. (1977). *Invariant Manifolds*. Springer LNM **583**.

Jorba, À. and Tatjer, J.C. (2005). On the fractalization of invariant curves in quasi-periodically forced 1-D systems. Preprint.

Keller, G. (1996). A note on strange nonchaotic attractors. *Fund. Math.* **151(2)**, pp. 139–148.

Mora, L. and Viana, M. (1993). Abundance of strange attractors. *Acta Math* **171**, pp. 1–71.

Osinga, H. and Feudel, U. (2000). Boundary crisis in quasiperiodically forced systems. *Physica D* **141(1-2)**, pp. 54–64.

Osinga, H., Wiersig, J., Glendinning, P. and Feudel, U. (2001). Multistability in the quasiperiodically forced circle map. *IJBC* **11**, pp. 3085–3105.

Palis, J. and Viana, M. (1994). High dimension diffeomorphisms displaying infinitely many periodic attractors. *Ann. of Math. (2)* **140(1)**, pp. 91–136.

Simó, C. (1979). On the Hénon-Pomeau attractor. *J. of Stat. Phys.* **21**, pp. 465–494.

Simó, C. (2003). On the use of Lyapunov exponents to detect global properties of the dynamics. *Proceedings Equadiff03*.

Tatjer, J.C. (2001). Three dimensional dissipative diffeomorphisms with homoclinic tangencies. *ETDS* **21(1)**, pp. 249–302.

Viana., M (1993). Strange attractors in higher dimensions. *Bol. Soc. Bras. Mat* **24**, pp. 13–62.

Viana., M (1997). Multidimensional nonhyperbolic attractors. *Publ. Math. IHES* **85**, pp. 63–96.

Vitolo, R. (2003). *Bifurcations of attractors in 3D diffeomorphisms*. PhD thesis, University of Groningen.

Wang, Q. and Young, L.-S. (2001). Strange Attractors with One Direction of Instability. *Comm. Math. Phys.* **218**, pp. 1–97.